A Hybrid SVM NAÏVE-BAYES Classifier for Bright Lesions Recognition in Eye Fundus Images

Nasr Gharaibeh[1], Obaida M. Al-hazaimeh[2], Ashraf Abu-Ein[1] and Khalid M.O. Nahar[3]

[1]Department of Electrical Engineering, Al-Balqa Applied University, Jordan
[2]Department of Computer Science, Al-Balqa Applied University, Jordan
[3]Department of Computer Sciences, Yarmouk University, Jordan
nas@bau.edu.jo, dr_obaida@bau.edu.jo, ashraf.abuain@bau.edu.jo, khalids@yu.edu.jo

Abstract: In recent years, much attention has been provided to developing the systems used for making medical diagnosis. That is because there are various developments made in the field of computing technology. The knowledge related to health and type of disease is essential for making a medical diagnosis by reliable and having an accurate detection. Regarding diabetic retinopathy (DR), it is a common cause for blindness. This disease can be detected in an early stage. It has various symptoms. The most distinctive symptoms are Micro-aneurysms (MAs), Hemorrhages (HAs) which are dark lesions and Hard Exudates (HEs), and Cotton Wool Spots (CWS) that are deemed as bright lesions. Through the present research, the researchers aimed at proposing an automated system for detecting exudates and cotton wool spots in an early stage and classifying them. Regarding the location of optic disc and the structure of blood vessels, they play a significant role in bright lesions for having the DR detected in an early stage. This paper presents algorithms and techniques for processing the retinal image, blood vessel segmentation and extraction, optic disc localization and removal, feature extraction and finally classification for different bright lesions using SVM and Naïve-Bayes classifiers. For testing retinal images, the researchers used image-Ret database which is a publicly available database. This database includes two sub-databases (i.e., DIARETDB0, and DIARETDB1). Finally, we compare the performance of recently published works and our proposed work.

Keywords: Fundus images; image processing; diabetic retinopathy; blood vessel segmentation; optic disc

1. Introduction

It should be noted that diabetic retinopathy (i.e., DR) is a considered a common retinal complication of diabetes. DR is the main cause for suffering from blindness among people of old and middle age groups [1, 2]. The International Diabetes Federation (i.e., IDF) declares that more than 50 million individuals in India suffer from this illness. It suggests that the number of ones who suffer from it has been increasing rapidly [3]. The estimated prevalence of diabetes worldwide among people of all age groups is represented by 2.8% in 2012. It is represented by 4.4% in 2030.Thus, it is expected that the number of diabetes patients shall rise to reach 366 million by the year 2030 [4]. The early detection of DR, it enables professionals to provide the patients with treatment on time. That shall reduce the severity of the consequences of this illness. To achieve early detection of diabetic retinopathy automated screening is necessary to avoid losing visions. DR is attributed to a problem in the vessels of the retina which is attributed to having an increase in the insulin level. Lesions in diabetic Fundus images have two types. One of those types is a bright lesion. Regarding the latter type, it involves cotton wool spots and exudates. The other one is a dark lesion that consists of micro-aneurysms and hemorrhages[1, 5]. It should be noted that those two types of lesions serve as signs of DR. Such signs reflect information on the early diabetic retinopathy and their associated features. Such lesions vary in terms of shapes, size, location, color, and texture. Micro-aneurysms manifest through red spots. They represent out pouching of the retinal capillaries. They are early signs of diabetic retinopathy [6]. Hemorrhages may manifest in large blots or small dots existing in the deep retina with severe cases. Regarding exudates, they manifest as white yellowish deposits that have lipo-protein edge

Received: October 29th, 2020. Accepted: August 30th, 2021
DOI: 10.15676/ijeei.2021.13.3.2

that is well defined. Exudates may be categorized into hard or soft ones. Regarding the soft ones, they are similar to cotton wool spots. The latter spots manifest as white grayish spots with fluffy edges that are poorly defined as Figures 1-2 are shown below in this regard [5, 7, 8].

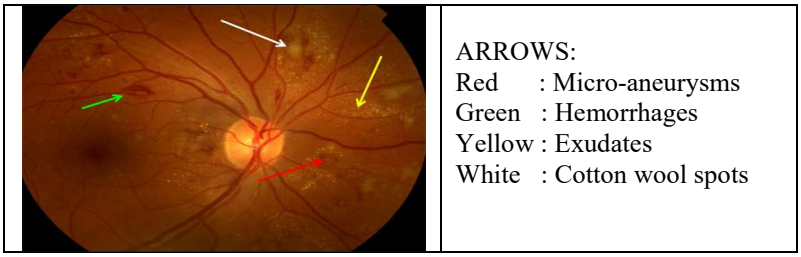

Figure 1. Diabetic retinopathy (Non-Proliferative)

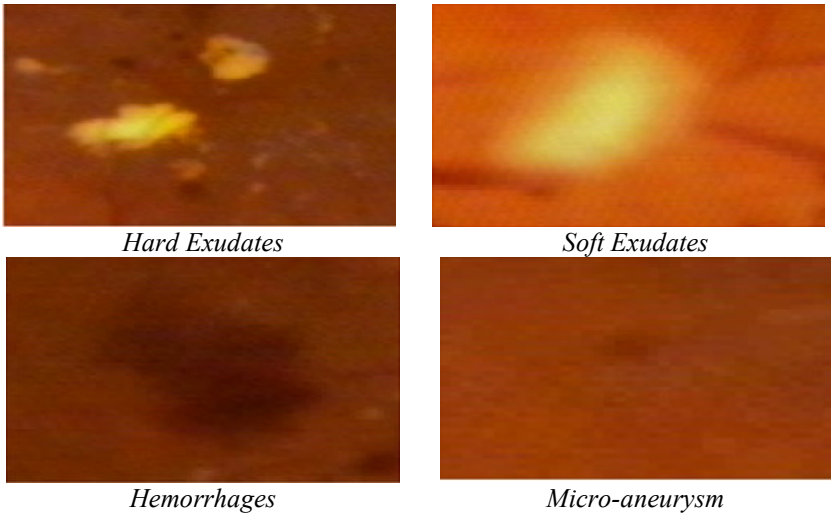

Figure 2. Lesions in diabetic retinopathy

Generally, DR has several stages. Such stages include: Proliferative Diabetic Retinopathy (i.e., PDR), Non-Proliferative Diabetic Retinopathy (i.e., NPDR), and macular edema (i.e., ME) or maculopathy. NPDR is widely known as the background DR. ME and PDR are signs of advanced stage among DR patients [9-11]. The three NPDR stages are summarized in Table 1.

Table 1. Stages of NPDR

Stage	**Description**
Mild	The mild signs manifest during the first stage of retinopathy. Some patients with mild signs have normal visions (Micro-aneurysms).
Moderate	During this stage, some blood vessels irrigate the retina. Some blood vessels shall become blocked. This stage precedes the severe stage. Hemorrhages are common among patients of moderate stage.
Severe	Cotton wool spots and exudates greatly occur in that stage. Additional vessels shall be blocked. Leakage might occur. However, leakage of blood can result in severe vision loss and even blindness.

This research includes five sections. The second section presents a review of the works that are related to DR. The 3rd section provides data on the system that is being proposed. The 4th section offers data on the experimental results. It presents data about the standard retinal image databases in which the researchers evaluated the proposed system. It presents the results of

conducting a trial on the proposed system and the results of conducting a comparison using various performance parameters and databases elaborated. The last section includes the conclusion.

2. Related Work

Diabetes may be called (disease). It leads to having abnormalities manifesting in the retina (i.e., DR). DR is a complication of a micro-vascular nature. It occurs due to suffering from diabetes. It may lead to blindness. During the early stages of DR, there aren't visible signs. However, the severity of DR can be identified through screening [12]. DR usually starts with having small changes to the retinal capillaries. Such changes are attributed to the abnormal changes that occurred to the retinal DR. For having an effective detection of illnesses (i.e., hemorrhages, exudates, micro-aneurysms, and cotton wool spots) in DR in an early stage, the objects in the retina image have three kinds, which are: the Bright lesions, dark lesions, and retinal background. Bright lesions include optic disk, cotton wool spots and exudates in a form of white or yellowish colors. Dark lesions include blood vessels, fovea, hemorrhages, and micro-aneurysms. The retinal background color ranges between dark and bright lesions [13].

The researchers reviewed the literature related to classifying and detecting diabetic retinopathy lesions (See [2, 4, 12, 14, 15]). However, many studies were conducted on the detection of dark lesion based on image processing. Such processing includes three major steps: pre-processing, lesion extraction, and classification (See[13]). Classifying bright lesions and detecting them through colored images and web-based automated detection were described in [16, 17].

Wisaeng et al. [18] developed a exudates detection methods in DR to segment color retinal images and provides high accuracy in exudates detection. Those methods include: Fuzzy C-Means clustering and morphological methods. This is not a final result of classification. However, the applications require higher accuracy values in segmentation results. For this reason, human ophthalmologists are essential for the cases in which the results of the detection aren't very clear. Another major disease is cotton wool spots. Such spots manifest due to having a fiber layer breaking from occlusion of pre-capillary arterioles. Early detection of cotton wool spots can prevent severe damage to retinal images affected by diabetic retinopathy [19]. Detecting the structures of the Fundus images (i.e., , fovea, optic disc and the retinal vessels)is essential in the automated detection of DR [20]. Rekhi et al. [21] developed automatic methods for detecting various lesions of diabetic retinopathy from the color retinal images. Hard exudates get detected by using a supervised learning method that is based on normal images. DR occurs due to having damage in one's vessels. It may lead to losing visions through micro-aneurysms [11].

Niemeijeret al [17] aimed to distinguish between the bright lesion (i.e. exudates, cotton wool spots, and drusen) from one hand and color retinal images from another hand. Through the first step, the pixels shall be classified. That shall lead to having the probability map. This map presents the probability of having every pixel becoming an element of the lesion that is bright. After that, the pixels that show much probability shall be categorized into groups into probable lesion pixel clusters. Depending on the characteristics of the clusters, each cluster shall be assigned a probability. This probability reflects the probability to which each cluster shall become a true bright lesion. At the end, those clusters shall be classified as cotton wool spots, exudates, and drusen. The researchers obtained the specificities and the sensitivities of the annotations on the three hundred images through the automated system. For bright lesion detection optic disc localization is necessary to perform in automated DR screening [22]. Sopharak et al. [23] use a key indicator of diabetic retinopathy which focuses on automatic exudates detection in Fundus images and then identifies exudates features by Naïve-Bayes classifier.

3. Proposed System

This research offers a system for the detection of DR from retinal Fundus images in an effective manner. To diagnose retinal images efficiently and effectively we have to contribute below mention processes. Our contributions are as follows,

- To reduce noises in a retinal image use local statistics which is executed in MATLAB using the wiener-2 function and enhance the contrast using CLAHE
- For bright lesion segmentation, we introduce MSW-FCM clustering algorithm
- To reduce features perform feature selection process based on US-PSO-RR algorithm
- To diagnose DR disease, we used SVM-MLC classifiers for classification.

Figure 3 presents the structure of the proposed system. Through this part, the detailed phases of the proposed system will be discussed.

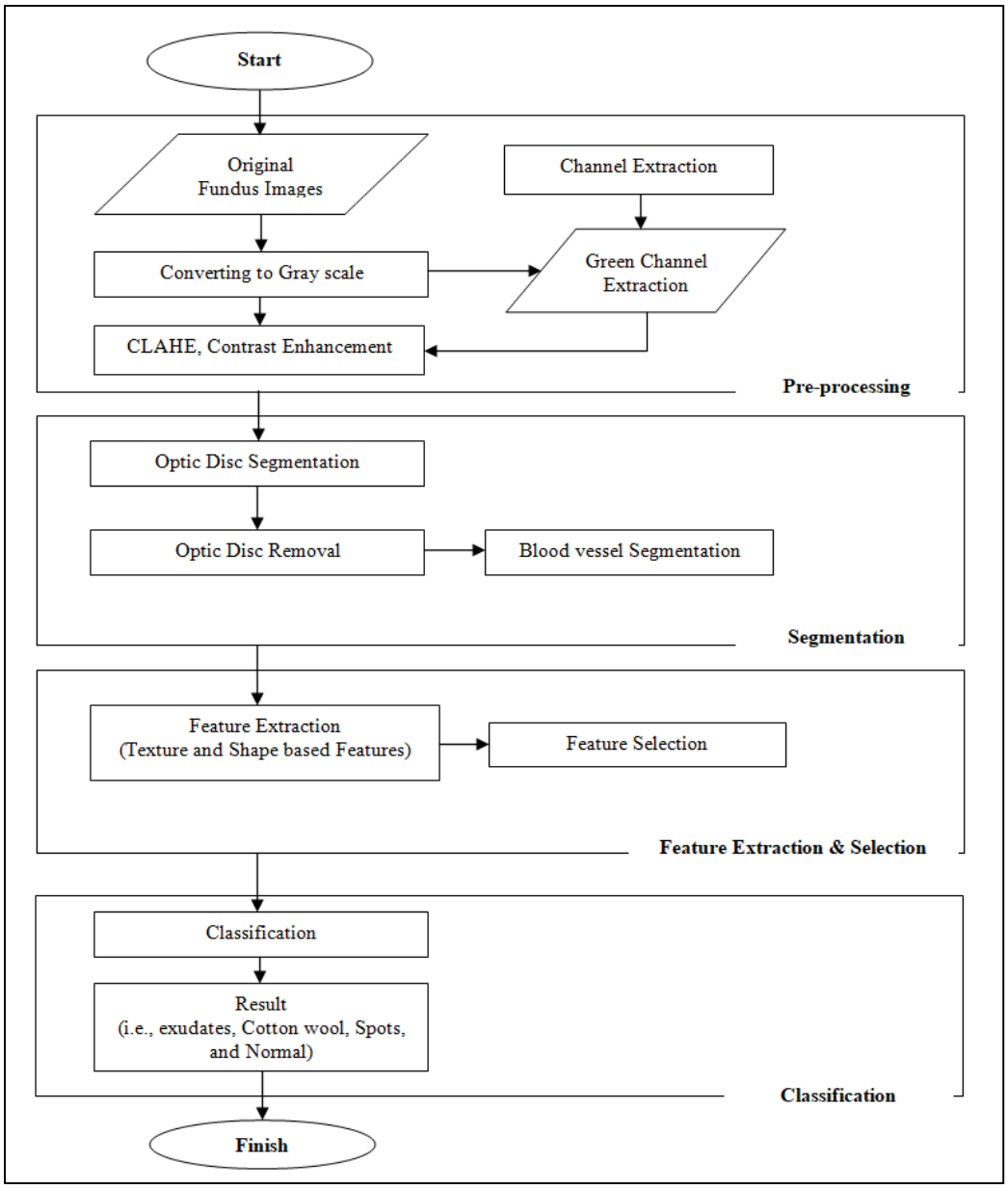

Figure 3. Proposed system architecture

A. Bright Lesions Detection

Bright lesions include exudates and cotton wool spots. They are deemed as the major DR symptoms. Early detection and classification of such diseases are very essential for providing patients with treatment that's considered effective [20]. This research offers an opportunity for applying the image processing approach to detect bright lesions and classify them. It offers brief information about the contemporary state of the algorithms used for image processing. Regarding the methods of image processing, they are categorized through Table 2.

Table 2. Methods of Image Processing

Method	**Functions**
Pre-processing	Normalization, intensity conversion, de-noising using logic statistics with wiener-2 function, and contrast enhancement using CLAHE
A modified canny edge detection algorithm	Localization and elimination for Optic disc
MSW-FCM	Segmentation and elimination for blood vessel
Haralick and shape-based features	Features extraction
US-PSO-RR	Features selection
MLC-SVM	Classification (i.e., Normal, or Cotton wool spots, or Exudates)

B. Pre-processing

Pre-processing is an essential step that must be employed before image segmentation. It is an improved technique for the image which suppresses undesired distortions or enhances some image features. There are various steps for pre-processing: normalization, intensity conversion, de-noising, and contrast enhancement. Below, we will recall the four pre-processing steps.

B.1. Normalization

To overcome the problems of the poor images intensity the normalization processing is performed. This process is carried out by applying a 30x30 median filter to subtract the background (i.e., approximate) from the gray image to produce a normalized image [24]. Median filtering is a non-linear method and it is very effective at removing noise while preserving edges. This method goes through the image pixel-by-pixel and replacing each considered pixels value with the median value (i.e., neighboring pixels). In other words, The median value is determined by sorting all the values of pixels from the window into numerical order, and then replacing the pixel being considered with the middle pixel value (i.e., median) [24].

B.2. Intensity Conversion

Usually, retinal images (i.e., Fundus images) are taken from databases and it shall be presented in RGB image. RGB image, it is converted into a grayscale image. The grey-scale image contains less information than a color image. But, most of the important feature-related information is maintained (i.e., junctions, blobs, edges, and regions) [2]. The latter image is formed using RGB pixel value by,

$$I_{gray-scale}(n,m) = \alpha\, I_{color}(n,m,r) + \beta\, I_{color}(n,m,g) + \gamma\ I_{color}(n,m,b) \quad (1)$$

where n and m are two individual pixels (i.e., indexes) within the grey-scale image.

B.3. De-noising

De-noising is mainly focused on the removal of noises present in the Fundus images. For that, we use local statistics with wiener-2-function. This function explicit in two ways: additive noise and multiplicative noise [25]. Here, we use additive noise for de-noising as given by,

denoising $image\ Y = X + n$ (2)

where *x* is a clear image and n is a noise to corrupted *x*.

B.4. Contrast Enhancement

Contrast enhancement is an important process that is used to correct uneven illumination and enhance the contrast of both RGB and grayscale images [26]. To overcome the drawback in histogram equalization, we proposed the BBHE method (i.e., Brightness Preserving Bi-Histogram Equalization). This method is used for the decomposition of original image into two sub-ones. That is done through the use of gray-level and a histogram equalization method on each image of the sub-images.

C. Optic Disc Detection and Removal

In Fundus images, optic disc (i.e., OD) is the brightest characteristic and color appearance of optic disc is bright yellow. Optic disc detection is the most important component for detecting exudates and cotton wool spots. That is because there is much similarity in terms of color and the contrast [19]. So we must detect OD and remove it in an efficient way for classifying exudates and cotton wool detection. Regarding the optic disc, they are similar to the structure of circular shape. Thus, in the present work, the researchers used a CHT technique (i.e., Circular Hough Transform) for OD detection. Hough transform is a shape-based approach in which shape of the OD is compared with a Hough circle. The main purpose of this circular transform method is represented in having tolerant gaps existing in the feature boundary description. Such gaps are not influenced much by the image noise [2]. OD circle can be defined as,

$$(x - a)^2 + (y - b)^2 + r^2 = 0 \quad (3)$$

b and *a* serve as the circle center in the direction of *x* and direction *y* with radius *r*. The OD circle parameters are:

$$x = a + r^* \cos(\theta), y = a + r^* \sin(\theta) \quad (4)$$

D. Blood Vessel Segmentation

This segmentation is the most significant task for effectively finding DR disease. Vessels serve as a landmark for localizing optic nerve, lesions, and fovea. They probably include abnormalities that are measurable in terms of color, diameter, and tortuosity [27]. Numerous segmentation algorithms are employed to segment the blood vessels in an accurate manner. Such techniques offer good results but don't contain any spatial information about the retinal images. To have the enhanced segments in the Fundus images extracted properly, a thresholding effective scheme is deemed essential. For that purpose, we introduce MSW-FCM algorithm (i.e., Modified spatial weighted fuzzy c-means). Through that method, the researchers compared the membership of central pixel with any one of the neighbor pixels in a window. Based on the results, they conducted an analysis to identify whether the central pixel is classified correctly or not. Regarding this spatial relationship, it is considered significant in clustering. The new spatial relationship function is given by,

$$S^*_{ij} = \sum_{k \epsilon H(x_j)} U_{ik} \beta_{k1} + \frac{\sum_{k \epsilon H(x_j)} U_{ik} \beta_{k2}}{\sum_{t=1}^{c} \sum_{k \epsilon H(x_j)} Utk} \quad (5)$$

H(xj) represents a square window centered on the pixel x_j in the spatial domain. The new spatial function has 2 coefficient parts: β_{k2} and $\beta_{k1}.\beta_{k1}$ Coefficient is caused by misclassified pixels from noisy regions which can get easily corrected in first parts. β_{k2} Coefficient is caused by membership function quantitative based on the distance between pixels. β_{k2} and β_{k1} are given by,

$$\beta_{k1} = \frac{1}{1 + \exp(\theta_1 ||j - k||)}, \beta_{k2} = \frac{1}{1 + \exp(\theta_2 ||xj - xk||)} \quad (6)$$

Regarding the spatial information, it is incorporated into membership function as given below,

$$U^{*}_{ij} = \frac{U_{ij}^{p} * S_{ij}^{*q}}{\sum_{k-1}^{c} U_{kj}^{p} * S_{ij}^{*q}} \quad (7)$$

where *i=1,2,…,c* and *j=1,2,…,n*. Choosing an objective appropriate function serves as the major key to having effective cluster analysis and obtaining clustering results of better quality. Regarding clustering optimization, it is based mainly on the function that's objective. For doing an objective suitable function, the researchers need to meet a set of requirements that are related to the distance between clusters from one hand and the data points that are assigned to the clusters from another hand. They need to meet requirements related to the distance between clusters that are minimized and maximized. FCM significantly shows low performance due to employing a prototype driven learning of parameter α at which α is based on exponential separation strength that exists between the clusters. α is represented by,

$$\alpha = \exp\left(-\min \frac{||v_i - v_k||2}{\beta}\right) \quad (8)$$

β stands for a normalized term which can be represented by,

$$\beta = \frac{\sum_{j=1}^{n} \left|\left|x_j - \bar{x}\right|\right| 2}{n} \; where, x^{-} = \frac{\sum_{j=1}^{n} x_j}{n} \quad (9)$$

The remark that must be identified in this context is represented in the common value *α* which is used in all the data and each iteration. This common value α may induce an error. The researchers proposed a new parameter. This parameter involves the common value α. It replaces *α* with a new parameter to each vector (i.e. weight of each vector). In the noisy data, this weight value leads to having a better classification level. Regarding the weight, it is calculated using the following formula,

$$W_{ji} = \frac{1}{1 + \exp\left(-\frac{\|x_j - v_i\|^2}{\sum_{j=1}^{n} \|x_j - \bar{v}\|^2 * \frac{c}{n}}\right)} \quad (10)$$

where W_{ji} is the weight of the point *j* in the relation to the class *i*. Regarding this weight, it is employed for modifying the typical and fuzzy partition**.** SW-FCM is represented as the given equation below,

$$MSW - FCM = \sum_{k=1}^{n} \sum_{i=1}^{c} \left(u_{ik}^{m} W_{ji}^{m}\right) |x_k - v_i|^2 \quad (11)$$

E. Feature Extraction

Feature extraction is used for classifying the segmented regions into cotton wool spots, exudates, and normal. They must be represented with significant and relevant features to give the best possible class separability [28]. The segmented regions (i.e., area of interest) can be differentiated through using several features (i.e., texture, size, edge, and color) as shown in Table 3.

Table 3. Area of Interest Feature

DR bright lesion	**Features**			
Lesions	**Color**	**Size**	**Shape**	**Edge**
Cotton Wool spot	Whitish	Medium - Small	Oval shape	Blur
Exudates	Yellowish	Small	Irregular	Sharp

19 features were extracted for each Fundus image in the proposed method. Regarding each feature, it can discriminate bright lesions from non-bright ones. Shape-based features are identified in the points as shown in Table 4.

Table 4. Shape-based Features

Feature	Equation	Variables description
Area	$A = \sum_{j \in \Omega} 1$	Ω is the pixel set in the bright regions.
Circularity	$C = \frac{p^2}{4\pi a}$	p represents the candidate bright lesion perimeter and a represents the bright lesion area.
Aspect ratio	$AR = \frac{L_1}{L_2}$	In covariance matrix, L_1 and L_2 are represents the length of the first and the second largest eigen vector.
Solidity	$S = A$	A is the area of the convex region
Region edge strength	$R\lvert\nabla f(a,b)\rvert = \sqrt{\left(\frac{\partial f}{\partial a}\right)^2 + \left(\frac{\partial f}{\partial b}\right)^2}$	R is the region edge strength

E.1. Texture based Features

Regarding Haralick texture features, they are based on distribution matrices (i.e., coarseness, homogeneity, periodicity, etc...) [29]. In terms of the details on the Haralick features, they are shown in the Table 5.

Table 5. Haralick Texture Features

Feature	Equation
Angular Second Moment (F_1)	$\sum_a \sum_b \{p(a,b)\}$
Contrast (F_2)	$\sum_{n=0}^{N-1} n^2 \left\{ \sum_{a=1}^{N} \sum_{B=1}^{N} p(a,b) \right\}$
Correlation (F_3)	$\frac{\sum_a \sum_b (ab)\, P(a,b) - \mu_x \mu_y}{\sigma_x \sigma_y}$
Sum of the squares (F_4)	$\sum_a \sum_b (a-\mu)^2 \; p(a,b)$
Inverse Difference Moment (F_5)	$\sum_a \sum_b \frac{1}{1+(a-b)^2} p(a,b)$
Sum Average (F_6)	$\sum_{a=2}^{2N} a p_{x+y(a)}$
Sum Variance (F_7)	$\sum_{a=2}^{2N} (a - f8)^2 p_{x+y}(a)$
Entropy (F_8)	$\sum_a \sum_b p(a,b) \log(p(a,b))$
Sum Entropy (F_9)	$\sum_{a=2}^{2N} p_{x+y}(a) \log\{p_{x+y}(a)\}$
Difference Variance (F_{10})	variance of p_{x-y}

Feature	Equation
Difference Entropy (F_{11})	$\sum_{a=0}^{N-1} p_{x-y}(a)\log\{p_{x-y}(a)\}$
Information of Measures of Correlation I (F_{12})	$(HXY - HXY1)/(\max\{HX, HY\})$
Information of Measure of correlation II (F_{13})	$(1\text{-}\exp[-2.0(HXY2\text{-}HXY)]^{1/2}$
Maximal Correlation Coefficient (F_{14})	(Second largest eigen value V)$^{1/2}$

F. Features Selection

This selection is a process that aims at selecting a subset of original features through the elimination of irrelevant features and/or redundant ones based on specific conditions[28, 30]. Relevant features were measured by discriminating the ability of a feature to enhance the predictive accuracy of classifier since it reduces the effect of noise which can efficiently describe the input data. In our proposed work we introduce the US-PSO-RR algorithm (i.e., Un-Supervised Particle Swarm Optimization based Relative Reduct) algorithm. Three steps are used in the following algorithm for feature selection.

Algorithm: Features Selection	
Input	Set of F (i.e., all conditional features)
Step 1:	Initialize V_n and X_n with random velocity and location respectively ∀: fit←0; Global_Best←fit;
Step 2:	While Fitness! = $\overline{\gamma_F}$(y) ∀y ∈ F For loop n=1,2,….S // ∀: X_n; T←{} Calculate the feature subset fitness (FSF) for X_n R← Subset feature of X_n(1's of X_n) ∀x∈ R; ∀y ∈ F $\gamma_{TU\|x\|}(y)=\frac{\|POS_{TU\|x(y)\|}}{\|U\|}$ FSF(n)=$\overline{\gamma_{TU\|x\|}(y)}$∀y ∈ F End_Loop structure
Step 3:	Calculate the best fitness: For loop n=1,2,….S If (FSF(n)>Global_Best) Global_Best←X_n; Global_Best←FSF(n); Location_Best (n)← Location_Best(X_n); Global_Best←X_n; If FSF(n)=$\overline{\gamma_F}$(y) ∀y ∈ F R←get Reduct (X_n) End_Conditions End_Loop strucure Update velocity of V_n's of X_n's Update location of X_n's
Output	Set of R (i.e., reducted features)

G. Features Classification

In our proposed approach, the classification process is done by using MLC (i.e., Maximum Likelihood Classifier) and SVM (i.e., Support Vector Machine) classifiers. These classifiers are commonly used in supervised machine learning. MLC is a parametric approach to estimate the probabilistic model and SVM is based on a non-parametric approach in optimization [27, 31]. In this paper, the combination between MLC and SVM is performed (i.e., SVM-MLC) for learning and classification. Below, we will recall the three stages of SVM-MLC.

G.1. Training and Classification-based Modeling

In feature extraction, there is some unknown and non-linear dependency between scalar output *y* and some high dimensional input vector *x* (i.e., y = f(x)) [32]. The goal is to separate

the images (i.e., normal, and abnormal) from the Image-Ret database. Generally, all training samples are given by,

$$Z=\{Z_l\}_{l=1}^{M} \ , Z_l \in R^m \tag{12}$$

where *M* is the training samples of *m* number of features.

G.2. Probability-based Modeling

In this stage, for calculating the related MLC models there are two classes (i.e., class 0 and class1) are used to lay all the samples which are correctly classified by SVM classifier. For robustness MLC models, the samples which cannot be correctly classified are ignored (i.e., outlier samples). For each sample *M* and the associated likelihoods (i.e., $P_0(M)$ and $P_1(M)$) that belongs to the classes, the classification decision is simplified as:

$$F_{MLC}(M) = \begin{cases} 1, & \text{if } P_1(M) - P_0(M) > \tau \\ 0, & \text{otherwise} \end{cases} \tag{13}$$

where τ is a threshold to generate the best-classified results (i.e., optimal).

G.3. Classification-based Improvement

Finally, all samples are re-assessed with the purpose to improve classification using the optimal threshold τ and the estimated MLC models.

4. Experimental Results

Our proposed bright lesions detection and classification of retinal disease processed using optic disc segmentation and removal, feature extraction, feature selection, and classification. Initially, pre-processing original retinal image by intensity conversion, reduce noise level using de-noising, and also performed contrast enhancement. Optic disc segmentation is done with the help of a Circular Hough Transform (i.e., CHT) technique. In this paper, the detection of the bright lesion is depicted in Figure 4.

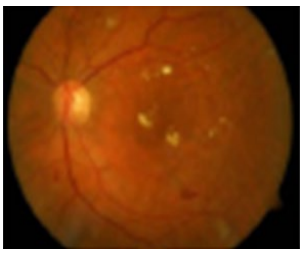

Fundus image

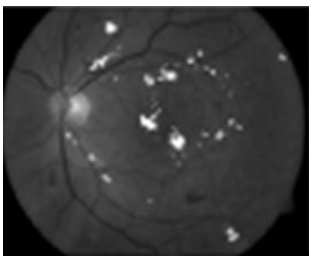

Bright Lesions

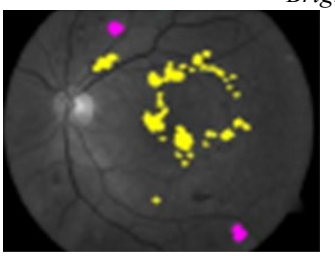

Exudates (Yellow) and cotton wool spots (Pink)

Figure 4. Lesions detection

For disease classification, in this paper, the researchers used SVM-MLC classifiers to increase the performance level (i.e., accuracy, sensitivity, and specificity).

A. Dataset

The image-Ret database is a publicly available database by Kauppi et al. in 2008 and it's divided into two groups (i.e., DIARETDB0, and DIARETDB1). The detailed specifications for each group are summarized in Table 6. The images were acquired with a 50^0 FOV (i.e., Field of View) using Fundus camera at a size of 1500*1152 pixels. To presence the retinal lesions(i.e., cotton wool spots, exudates, and normal), the images were annotated by three expert people [33]. In this database, images of exudates and cotton wool spots are automatically annotated by classifiers, which can be used to evaluate the proposed method.

Table 6. Image-Ret database

Dataset	**Normal.PNG**	**Abnormal.PNG**	**Total**
DIARETDB0	20	110	130
DIARETDB1	5	84	89

B. Performance Metrics

To measure the correct classification and detection rate (i.e., performance level) of the proposed method, such metrics include: sensitivity (i.e., recall), accuracy, and specificity are commonly used [2, 34]. These metrics are reported in Table 7.

Table 7. Performance Metrics

Metric	**Equation**
Specificity	$TN/(TN+FP)$
Accuracy	$(TP+TN)\ /\ (TP+TN+FP+FN)$
Sensitivity	$TP/(TP+FN)$

C. Comparative Analysis

In our experiments, the analysis of classification and segmentation are presented through comparing the performance of the optic disc detection methods. But, before conducting a comparison process between these methods, the researchers presented the results of each stage (i.e., pre-processing, optic disc segmentation and removal) as shown in Figures 5 and 6.

Original image

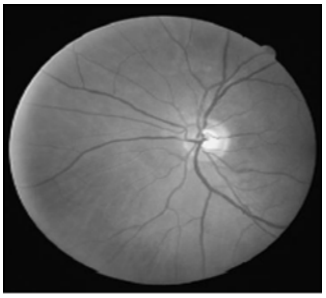

De-noising image

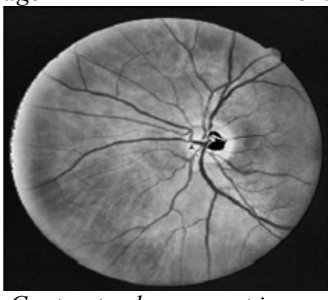

Contrast enhancement image

Figure 5. Pre-processing stage

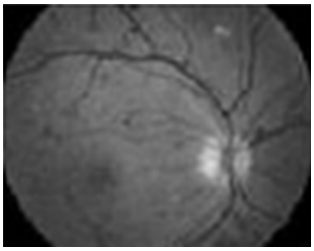

Optic disc segmentation

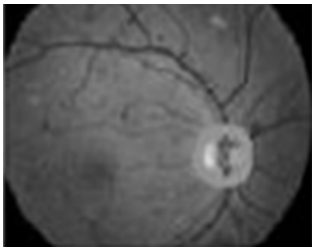

Optic disc detection

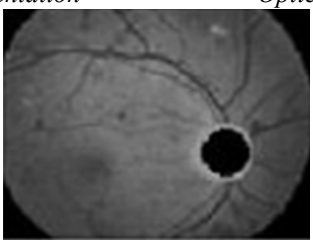

Optic disc elimination

Figure 6. Optic disc segmentation and removal stage

Moreover, the blood vessels are detected in this paper and then segmented using MSW-FCM. The results of blood vessel detection and segmentation can be depicted in Figure 7.

Input image

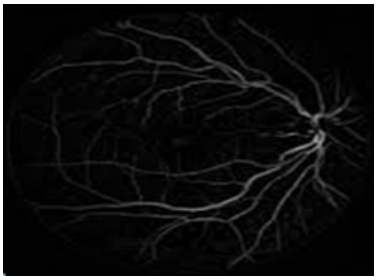

Segmented blood vessel

Figure 7. Blood vessel segmentation

Segmentation accuracy is calculated in accordance with the selected metrics of performance. It is measured through making a comparison with some existent works (i.e., state-of-the-art). In this research, the comparison results for Optic disc localization are listed in Table 8. The column chart diagram for the comparison process between classifiers is displayed in Figure 8.

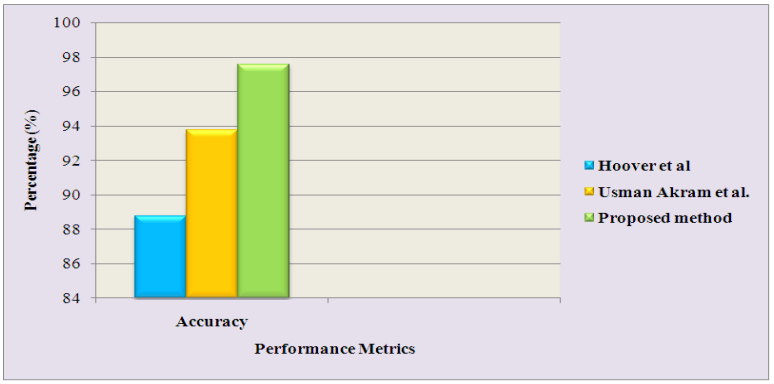

Figure 8. State-of-the-art comparison result

Table 8. Comparison Results

Method	Total images	Successful Localization	Failed Localization	Accuracy (%)
Hoover et al.[35]	81	72	9	88.8
Akram et al.[36]	81	76	5	93.8
Proposed method	219	212	7	96.80

Moreover, a comparison is carried out in this paper between PNN, KNN, SVM classifiers and the proposed SVM-MLC classifier in terms of the metrics of performance (i.e., specificity, sensitivity, and accuracy). The comparison results are shown through Table 9. To make it clearer, the column chart diagram for the comparison process is displayed in Figure 9.

Table 9. Comparison-based Performance Metrics

Classifier	Sensitivity	Specificity	Accuracy
SVM-MLC	99 %	99 %	98.60 %
PNN	90 %	98 %	89.6 %
KNN	95.6 %	94.87 %	95.38 %
SVM	98 %	96 %	97.6 %

Figure 9. Comparison results

5. Conclusion

The proposed method aims at detecting exudates and cotton wool spots. The overall process for disease detection is pre-processing, optic disc localization and removal, vessel segmentation, feature extraction, feature selection, and classification. The problem with Fundus images is that the detection and elimination of optic disc. Due to this problem, lesions detection is a very challenging task in DR. The researchers tested the proposed method on DIARETDB0 and DIARETDB1 databases that are publicly available. Generally, all processes must improve sensitivity, specificity, and accuracy at the diagnosis of DR diseases (i.e., exudates and cotton wool spots). Our proposed system helps in automatic disease detection purposes and will produce better results in optic disc localization and classification. Finally, the proposed system show high sensitivity (99%). It shows high specificity (99%) and high accuracy (98.60%). The researchers decided to plan to use some other classifiers and expand the dataset in databases in the future to improve the accuracy of the processes that aim at detecting exudates and cotton wool spots.

6. References

[1] Z. Xiaohui and A. Chutatape, "Detection and classification of bright lesions in color fundus images," in *2004 International Conference on Image Processing, 2004. ICIP'04.*, 2004, pp. 139-142.

[2] N. Gharaibeh, O. M. Al-Hazaimeh, B. Al-Naami, and K. M. Nahar, "An effective image processing method for detection of diabetic retinopathy diseases from retinal fundus images," *International Journal of Signal and Imaging Systems Engineering,* vol. 11, pp. 206-216, 2018.

[3] S. Joshi and P. Karule, "A review on exudates detection methods for diabetic retinopathy," *Biomedicine & Pharmacotherapy,* vol. 97, pp. 1454-1460, 2018.

[4] D. Devaraj, R. Suma, and S. P. Kumar, "A survey on segmentation of exudates and microaneurysms for early detection of diabetic retinopathy," *Materials Today: Proceedings,* vol. 5, pp. 10845-10850, 2018.

[5] J. H. Tan, H. Fujita, S. Sivaprasad, S. V. Bhandary, A. K. Rao, K. C. Chua*, et al.*, "Automated segmentation of exudates, haemorrhages, microaneurysms using single convolutional neural network," *Information sciences,* vol. 420, pp. 66-76, 2017.

[6] S. Yu, D. Xiao, and Y. Kanagasingam, "Exudate detection for diabetic retinopathy with convolutional neural networks," in *2017 39th Annual International Conference of the IEEE Engineering in Medicine and Biology Society (EMBC)*, 2017, pp. 1744-1747.

[7] H. Yazid, H. Arof, and N. Mokhtar, "Edge sharpening for diabetic retinopathy detection," in *2010 IEEE Conference on Cybernetics and Intelligent Systems*, 2010, pp. 41-44.

[8] Y.-P. Liu, Z. Li, C. Xu, J. Li, and R. Liang, "Referable diabetic retinopathy identification from eye fundus images with weighted path for convolutional neural network," *Artificial intelligence in medicine,* vol. 99, p. 101694, 2019.

[9] S. Guo, K. Wang, H. Kang, T. Liu, Y. Gao, and T. Li, "Bin loss for hard exudates segmentation in fundus images," *Neurocomputing,* vol. 392, pp. 314-324, 2020.

[10] N. Thomas and T. Mahesh, "Detecting clinical features of diabetic retinopathy using image processing," *International Journal of Engineering Research & Technology (IJERT),* vol. 3, pp. 558-561, 2014.

[11] I. Usman and K. A. Almejalli, "Intelligent Automated Detection of Microaneurysms in Fundus Images Using Feature-Set Tuning," *IEEE Access,* vol. 8, pp. 65187-65196, 2020.

[12] M. B. Patwari, R. R. Manza, Y. M. Rajput, M. Saswade, and N. K. Deshpande, "Review on detection and classification of diabetic retinopathy lesions using image processing techniques," *International Journal of Engineering Research & Technology (IJERT), ISSN,* pp. 2278-0181, 2013.

[13] H. Poostchi, S. Khakmardan, and H. Pourreza, "Diabetic retinopathy dark lesion detection: preprocessing phase," in *2011 1st International eConference on Computer and Knowledge Engineering (ICCKE)*, 2011, pp. 177-182.

[14] M. Akter and M. S. Uddin, "A review on automated diagnosis of diabetic retinopathy," *Compusoft,* vol. 3, p. 1161, 2014.

[15] I. Qureshi, J. Ma, and Q. Abbas, "Diabetic retinopathy detection and stage classification in eye fundus images using active deep learning," *Multimedia Tools and Applications,* vol. 80, pp. 11691-11721, 2021.

[16] X. Zhang and O. Chutatape, "Top-down and bottom-up strategies in lesion detection of background diabetic retinopathy," in *2005 IEEE Computer Society Conference on Computer Vision and Pattern Recognition (CVPR'05)*, 2005, pp. 422-428.

[17] M. Niemeijer, B. van Ginneken, S. R. Russell, M. S. Suttorp-Schulten, and M. D. Abramoff, "Automated detection and differentiation of drusen, exudates, and cotton-wool spots in digital color fundus photographs for diabetic retinopathy diagnosis," *Investigative ophthalmology & visual science,* vol. 48, pp. 2260-2267, 2007.

[18] K. Wisaeng, N. Hiransakolwong, and E. Pothiruk, "Automatic detection of exudates in diabetic retinopathy images," *Journal of Computer Science,* vol. 8, p. 1304, 2012.

[19] P. Prentašić and S. Lončarić, "Detection of exudates in fundus photographs using deep neural networks and anatomical landmark detection fusion," *Computer methods and programs in biomedicine,* vol. 137, pp. 281-292, 2016.
[20] K. Noronha and K. P. Nayak, "Fundus image analysis for the detection of diabetic eye diseases-a review," in *2012 International Conference on Biomedical Engineering (ICoBE)*, 2012, pp. 242-246.
[21] R. S. Rekhi, A. Issac, M. K. Dutta, and C. M. Travieso, "Automated classification of exudates from digital fundus images," in *2017 International Conference and Workshop on Bioinspired Intelligence (IWOBI)*, 2017, pp. 1-6.
[22] M. M. Fraz, W. Jahangir, S. Zahid, M. M. Hamayun, and S. A. Barman, "Multiscale segmentation of exudates in retinal images using contextual cues and ensemble classification," *Biomedical Signal Processing and Control,* vol. 35, pp. 50-62, 2017.
[23] A. Sopharak, B. Uyyanonvara, and S. Barman, "Automatic microaneurysm detection from non-dilated diabetic retinopathy retinal images using mathematical morphology methods," *IAENG International Journal of Computer Science,* vol. 38, pp. 295-301, 2011.
[24] W. Zhou, C. Wu, Y. Yi, and W. Du, "Automatic detection of exudates in digital color fundus images using superpixel multi-feature classification," *IEEE Access,* vol. 5, pp. 17077-17088, 2017.
[25] B. Ramasubramanian and G. Mahendran, "An efficient integrated approach for the detection of exudates and diabetic maculopathy in colour fundus images," *Advanced Computing,* vol. 3, p. 83, 2012.
[26] A. G. Marupally, K. K. Vupparaboina, H. K. Peguda, A. Richhariya, S. Jana, and J. Chhablani, "Semi-automated quantification of hard exudates in colour fundus photographs diagnosed with diabetic retinopathy," *BMC ophthalmology,* vol. 17, pp. 1-9, 2017.
[27] H.-Y. Tsao, P.-Y. Chan, and E. C.-Y. Su, "Predicting diabetic retinopathy and identifying interpretable biomedical features using machine learning algorithms," *BMC bioinformatics,* vol. 19, p. 283, 2018.
[28] O. M. Al-Hazaimeh, M. Al-Nawashi, and M. Saraee, "Geometrical-based approach for robust human image detection," *Multimedia Tools and Applications,* vol. 78, pp. 7029-7053, 2019.
[29] S. Simonthomas, N. Thulasi, and P. Asharaf, "Automated diagnosis of glaucoma using Haralick texture features," in *International Conference on Information Communication and Embedded Systems (ICICES2014)*, 2014, pp. 1-6.
[30] M. Al-Nawashi, O. M. Al-Hazaimeh, and M. Saraee, "A novel framework for intelligent surveillance system based on abnormal human activity detection in academic environments," *Neural Computing and Applications,* vol. 28, pp. 565-572, 2017.
[31] O. Al-Hazaimeh and M. Al-Smadi, "Automated Pedestrian Recognition Based on Deep Convolutional Neural Networks," *International Journal of Machine Learning and Computing,* vol. 9, pp. 662-667, 2019.
[32] H.-r. Li, F.-z. He, and X.-h. Yan, "IBEA-SVM: an indicator-based evolutionary algorithm based on pre-selection with classification guided by SVM," *Applied Mathematics-A Journal of Chinese Universities,* vol. 34, pp. 1-26, 2019.
[33] T. Kauppi, V. Kalesnykiene, J.-K. Kamarainen, L. Lensu, I. Sorri, J. Pietila*, et al.*, "DIARETDB1-standard diabetic retino-pathy database," *IMAGERET-Optimal Detect. Decis. Diagnosis Diabet. Retin.,* pp. 15.1-15.10, 2007.
[34] M. A.-H. Obaida, "Combining audio samples and image frames for enhancing video security," *Indian Journal of Science and Technology,* vol. 8, p. 940, 2015.
[35] A. Hoover and M. Goldbaum, "Locating the optic nerve in a retinal image using the fuzzy convergence of the blood vessels," *IEEE transactions on medical imaging,* vol. 22, pp. 951-958, 2003.
[36] M. U. Akram, S. Khalid, and S. A. Khan, "Identification and classification of microaneurysms for early detection of diabetic retinopathy," *Pattern Recognition,* vol. 46, pp. 107-116, 2013.

Nasr Gharaibeh is an Assistance Professor in the Department of electrical Engineering. Now, he is a lecturer at Al-Balqa Applied University – Al-Huson University College, Jordan.

Obaida M. Al-Hazaimeh is an Associate Professor in Computer Science. He received his BS in Computer Science from Applied Science University (ASU), Jordan in 2004, the MSc in Computer Science from University Science Malaysia (USM), 2005, and PhD in Computer Science in 2010. Now, he is a Lecturer at Al-Balqa Applied University – Al-Huson University College, Jordan.

Ashraf Abu-Ein is an Associate Professor in the Department of electrical Engineering. Now, he is a lecturer at Al-Balqa Applied University – Al-Huson University College, Jordan.

Khalid M.O. Nahar is an Associate Professor in the Department of Computer Sciences-Faculty of IT, Yarmouk University, Irbid-Jordan. He received his BS and MS in Computer Sciences from Yarmouk University in Jordan, in 1992 and 2005, respectively. He was awarded a full scholarship to continue his PhD in Computer Sciences and Engineering from King Fahd University of Petroleum and Minerals (KFUPM), KSA.